IMPROVED PSO ALGORITHM APPLICATION RESEARCH FOR NEW ENERGY CONSUMPTION IN MICROGRID COMBINATION OPTIMISATION MODEL

Guodong Wu*,** Diangang Hu,** Lijuan Liu,*** and Guangqing Bao*

Abstract

With the rapid development of new energy technology, how to effectively integrate and consume these energy sources has become a major challenge for power grid scheduling and management. To solve the optimisation problem of new energy consumption in microgrids (Mgs), this study proposes to improve the particle swarm optimisation (PSO) algorithm and apply it to the Mg combination optimisation model. Based on the PSO algorithm, a simulated annealing (SA) algorithm is introduced to construct a SA particle swarm algorithm for new energy consumption. At the same time, combined with a Mg example in a certain city in China, a comparison was made through experiments with multi-objective PSO (MOPSO), traditional particle swarm algorithm, and sparrow search algorithm (SSA). The experimental results showed that the SAPSO algorithm ensured that the new energy consumption rate of the Mg system reached 100%, to achieve the effect of environmental protection and energy conservation. The research results of this study have achieved the economic and environmental goals of Mg operation while meeting user load demands and have played an important role in the field of new energy consumption. The study optimised the consumption plan of new energy, improved the utilisation rate of renewable energy, reduced the operating cost of Mg systems, and provided important theoretical and practical guidance for Mg management.

* College of Electrical and Information Engineering, Lanzhou University of Technology, Lanzhou, 730050, China; e-mail: wuguodong0943@126.com; baogq03@163.com
** State Grid Gansu Electric Power Company, Lanzhou, 730030, China; e-mail: hudg_163@163.com
*** State Grid Gansu Electric Power Company Electric Power Science Research Institute, Lanzhou, 730030, China; e-mail: 18294452085@163.com
Corresponding author: Diangang Hu

Key Words

New energy consumption, particle swarm optimisation, microgrid, optimisation, model

1. Introduction

Microgrid (Mg) has the advantages of autonomy, reliability, and sustainability, which can realise flexible scheduling of renewable energy [1]. However, operation scheduling and optimisation of Mg are facing challenges, such as complexity and multi-objective, which need to find effective optimisation methods to solve. The common combinatorial mathematical model refers to the standard mathematical model widely used in the branch of combinatorial mathematics to solve various permutation and combination problems. These models are commonly used to study the ordered or unordered combination, selection, arrangement, and other problems of elements under specific specified conditions. Common combinatorial mathematical models are used to calculate probabilities, optimise, and solve scheduling problems, and are widely applied in computer science, physics, operations research, and many other fields. The combinatorial optimisation model refers to the combinatorial optimisation problem of multiple energy sources in Mg systems. The goal of the combinatorial optimisation model is to find the optimal energy combination scheme to meet the needs of the Mg system, maximise energy utilisation efficiency, reduce energy costs, or reduce dependence on traditional energy sources. With the increasing proportion of renewable energy in the energy supply, Mg, as a small and highly intelligent energy system, has become increasingly important. However, due to the instability and intermittency of renewable energy, how to better integrate and absorb new energy has become an important issue

in Mg management. Therefore, the motivation of this study is to find an optimisation model to better manage and absorb new energy and improve the reliability and economy of Mgs. As a heuristic optimisation algorithm, the particle swarm optimisation algorithm (PSO) has a simple implementation [2]. In Mg operation, PSO can solve the combinatorial optimisation problem of Mg. The traditional PSO algorithm often suffers from premature convergence and is prone to getting stuck in local optimal solutions. To address this issue, this study introduces several objective functions: a minimum cost function that considers the economy of Mg, an operation cost function focusing on environmental protection, an objective function that balances both economy and environmental protection, and an objective function for energy consumption of micro gas turbines (MT). To solve the optimisation problem of Mg combination, an improved PSO for new energy consumption is proposed using PSO and simulated annealing (SA), which is applied to the optimisation of Mg.

This study includes four parts. The first part is the research results of domestic and foreign scholars on Mg and its combined optimisation. The second part discusses the common mathematical model of Mg combination, proposes the objective function in Mg combination, and constructs an improved SAPSO to solve the objective function. In the third part, the algorithm is tested and applied to an example for analysis. The fourth part summarises the article and points out the shortcomings.

2. Related Works

Mg is a distributed energy system, which can not only operate independently but also connect with the main grid to balance energy supply and demand. Some experts have done relevant research on Mg. Le and Phung found that when the Mg operated in island mode, faults may occur. Therefore, in consideration of sustainable power supply, the frequency was restored to the allowable range through the primary and secondary adjustment of the generator. The PSO determined the distributed disconnection power to improve the voltage quality [3]. Ndukwe et al. proposed a Lora-based wireless communication system for Mg data transmission. The system allowed multiple sensors to be connected to Lora transceivers and collected data from various units in the Mg. By testing the data transmission efficiency, wireless communication system effectiveness was verified [4]. To solve Mg's security problem, Cepeda et al. proposed an intelligent fault detection system for Mg based on local measurement and machine learning technology. By integrating the ML system, each smart electronic device in the Mg can detect faults independently. Through the analysis of simulation experiments, the effectiveness of this method was proved [5]. An et al. found that electric vehicles can alleviate the peak load, transmission, and storage problems of the Mg by deploying the Internet of Things. To solve personal information leakage, an online location privacy protection scheme was proposed. This scheme can distribute the power and charging stations in the Mg to

electric vehicles in the case of a limited energy supply. Results showed good effectiveness [6].

By solving the Mg combinatorial optimisation problem, the balance among power system cost, efficiency, and environmental protection can be achieved. Some experts have made relevant achievements on the combinatorial optimisation problem of Mg. Masuda et al. studied the operation and demand response of Mg. The scheme applied the distributed asynchronous primal-dual algorithm to deal with the communication delay and update delay of some subsystems, and algorithm effectiveness was proved [7]. Ghaemi and Salehi found that renewable energy increased net load variability in Mg, so the system may have the problem of power interruption. Based on this, considering the limitations of investment, the benders decomposition method solved the problem in the system. Experiments showed that this method can reduce system cost and achieve new energy maximum output [8]. Krishna et al. found that as renewable energy spread, the uncertainty of power generation in Mg needed to be solved. However, Mg dispatch and planning were affected by the volatility of renewable energy, load demand, and price. Based on this, taking renewable energy, user load demand, and price as the objective function, the decision tree can solve the problem. Experiments showed that it can realise Mg combinatorial optimisation [9]. Zeinal-Kheiri et al. proposed a new Mg system in view of the uncertainty caused by the prediction errors of renewable energy generation, load, and market price in Mg. The system solved this problem by defining different virtual queues to meet the time coupling constraints. The results showed that this system can well improve the combinatorial optimisation in Mg [10].

Using PSO combined with ANISN code, Wu et al. proposed a multi-objective optimisation method for the design of lightweight radiation shielding in nuclear reactors and verified its reliability through MCNP. The results indicated that this method effectively improved the quality of the shielding scheme [11]. Using the PSO algorithm, Abbaszadeh et al. proposed a new parameter optimisation method for the SVC model selection problem and successfully applied it to the geological modelling of the Yiju porphyry copper deposit. The results showed that this method effectively improved the accuracy of identifying alteration and mineralisation zones and was superior to traditional grid search methods [12]. Using BP neural network and multipole coupling theory, Chen et al. proposed a structural parameter optimisation method for optimising the spectral performance of all-dielectric sub-surfaces, and improved Fano resonance using genetic algorithm, sparrow search algorithm (SSA), and PSO algorithm. The results showed that PSO significantly improved the quality factor and achieved high modulation depth, providing a new optimisation strategy for optical micro/nanostructure design [13].

To sum up, most of the existing research focuses on the Mg itself, while there is a lack of intelligent solution algorithms for the Mg combinatorial optimisation problem. Therefore, based on PSO, this study introduces SA for PSO optimisation. Based on the SAPSO, the Mg combinatorial optimisation problem under the new
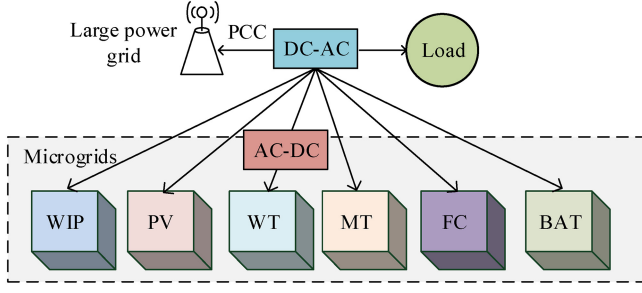
Figure 1. Structure diagram of microgrid model.

energy consumption is solved to achieve the balance of cost and environmental protection in the Mg operation. The improved PSO algorithm proposed in this study has made significant improvements in parameter adjustment and optimisation strategies to enhance the algorithm's adaptability and convergence speed, especially in the face of complex high-dimensional problems, exhibiting higher efficiency and stability. Thus, in solving optimisation problems with dynamic changes, research methods fill the existing research gap, and provide new perspectives in both theory and practice.

3. Microgrid Combination Optimisation Model Construction

To achieve optimal solution calculation of the objective function of Mg combination cost, environmental protection, comprehensive benefits, and energy consumption under the new energy consumption, this chapter is divided into three parts to build the combination optimisation model. The first part discusses the common combined mathematical model of Mg, which paves the way for the construction of subsequent models, the second part proposes the objective function of Mg combination, and the third part constructs an improved SAPSO to solve the objective function.

3.1 Microgrid Combination Mathematical Model

Mg is a distributed energy system composed of traditional power generation energy, new energy, and energy storage equipment in a specific geographical area. The Mg can operate independently and can also be interconnected with the main grid to achieve mutual interaction of energy and balance of supply and demand. By combining renewable energy with traditional power generation, Mg can better cope with the volatility and uncertainty of energy supply. The grid-connected Mg includes three elements: micro power supply device, user load, and energy storage device. The Mg model structure is shown in Fig. 1.

Micro power devices include photovoltaics (PV), wind turbine (WT), MT, fuel cell (FC), and waste incineration power plant (WIP). The energy storage device is mainly lead acid batteries (BAT), and the load is mainly the power demand of users' daily life. PV system converts light energy into electric energy through semiconductor materials, but the daily sunshine intensity is different, so the power generation by light energy has fluctuation. PV

system output power is shown in (1) [14].

$$P_{\text{PV}} = f_{\text{PV}} Y_{\text{PV}} \frac{I_T}{I_S} [1 + \alpha_p (T_{\text{cell}} - T_{\text{cell,STC}})] \quad (1)$$

In (1), P_{PV} is the PV output power, f_{PV} is the power derating factor, Y_{PV} is the capacity of PV, I_T and I_S are the solar irradiation intensity, α_p is the power temperature coefficient, and T_{cell} and $T_{\text{cell,STC}}$ are the PV panel surface temperature. WT is also a kind of renewable energy power generation technology, and its power output is proportional to wind speed (WS). WT system output power is shown in (2) [15].

$$P_{\text{WT}} = \begin{cases} 0 & 0 \leq v \leq v_{\text{ci}} \\ P_N \frac{v - v_{\text{ci}}}{v_N - v_{\text{ci}}} & v_{\text{ci}} \leq v \leq v_N \\ P_N & v_N \leq v \leq v_{\text{CO}} \\ 0 & v_{\text{CO}} \leq v \end{cases} \quad (2)$$

In (2), P_{WT} refers to WT output power and P_N is the output power under rated WS. v represents the actual WS, v_{ci} represents the cut-in WS, v_{CO} represents the cut-out WS, and v_N represents the rated input WS. Therefore, when the WS is greater than 0 and less than the cut in WS, WT will not generate electricity. When WS is less than the cut, WT also does not generate electricity. When the WS is greater than the cut in WS and less than the rated WS, WT is proportional to the WS. The MT system uses methane, natural gas, or fuel oil and air as the medium, which is different from the traditional diesel generator and has high efficiency and low pollution. Since the amount of fuel and air entering the MT is controllable, the optimal operation method of the Mg can be calculated manually. During grid-connected operation, the output power of WT is stable after reaching a stable working state, as shown in (3) [16].

$$P_{\text{MT}} = 0.000293 Q_f (\text{HV})_s \eta_t \left(\frac{\text{PS}}{PS_S} \right) \left(\frac{T_S}{T} \right) \quad (3)$$

In (3), P_{MT} represents WT actual output power, Q_f is the fuel gas flow rate, and $(\text{HV})_s$ is the fuel gas heat rate at standard temperature and standard atmospheric pressure. η_t represents WT total efficiency, PS represents the gas pressure value, PS_S represents the standard pressure, T_S represents the standard temperature, and T represents the actual temperature. FC can convert chemical energy in fuel and oxidants into electric energy at a constant temperature. Hydrogen-rich gas, liquid, CO, or gas are usually used as fuel. FC has no mechanical parts, so it has high conversion efficiency and less harmful gas emissions. Hydrogen energy is a kind of clean energy, so the regulation of FC is also a work of combinatorial optimisation. The output of FC is shown in (4) [17].

$$\begin{cases} U_{\text{FC}} = N_{\text{cell}} N_S U'_{\text{FC}} \\ I_{\text{FC}} = N_S I'_{\text{FC}} \\ P_{\text{FC}} = U_{\text{FC}} I_{\text{FCo}} \end{cases} \quad (4)$$

In (4), U_{FC} and I_{FC} represent FC output voltage and current, P_{FC} represents FC output power, N_{cell} represents the number of each group of FC, N_S represents the number of FC groups. U'_{FC} and I'_{FC} represent the output voltage and current of a single FC. WIP system mainly includes feeding equipment, incinerators, and purification equipment. The purification equipment can treat the pollutants in the incinerator to achieve the purpose of pollution-free emissions. The output power of WIP is shown in (5) [18].

$$P_{\text{WIP}} = \mu_{\text{WIP}} G_{\text{WIP}} \tag{5}$$

In (5), P_{WIP} is the WIP output power, μ_{WIP} is the factor of converting waste per unit into electric energy, and G_{WIP} is the waste weight per unit. There are two kinds of energy storage devices in Mg, namely, chemical energy storage and physical energy storage. Bat is a kind of chemical energy storage device, which has low cost and wide application on the premise of ensuring the consumption of new energy. Bat power is shown in (6) [19].

$$S_{\text{SOC}}(t+1) = S_{\text{SOC}}(t) - \frac{E_{\text{BAT}}(t)}{V_{\text{BAT}}} \tag{6}$$

In (6), $S_{\text{SOC}}(t+1)$ represents the battery storage power at the next time and $S_{\text{SOC}}(t)$ is the battery storage power at t. $E_{\text{BAT}}(t)$ indicates the charge and discharge capacity of BAT in the t period. A positive value indicates discharge, a negative value indicates charge, and V_{BAT} indicates the total capacity of BAT.

3.2 Mg Portfolio Optimisation Model Construction for New Energy Consumption

In Mg operation, the power generation of PV and WT systems is uncontrollable, and the cost of the system will decrease sharply for every one percentage point increase in the utilisation rate of PV and wt. Because higher utilisation often means higher energy output, this can lower overall system costs by reducing the demand for other more expensive energy sources. Therefore, finding an optimal technical and economic balance point will be an important measure to improve the new energy utilisation rate. Taking into account the fuel, maintenance, equipment, and interaction cost of the Mg system, the minimum cost objective function considering only the Mg economy is obtained as shown in (7) [20].

$$\min C_1 = \sum_{t=1}^{T} (C_f(t) + C_{\text{ma}}(t) + C_{\text{dep}}(t) + kC_{\text{grid}}(t)) \tag{7}$$

In (7), $\min C_1$ refers to the Mg operation cost with the economy as a goal, $\sum_{t=1}^{T}(\cdot)$ is the sum of daily consumption costs, and $C_f(t)$ is the fuel consumption cost at time t, in kWh. $C_{\text{ma}}(t)$ represents the equipment maintenance cost, $C_{\text{dep}}(t)$ represents the depreciation loss of each power unit, and $kC_{\text{grid}}(t)$ represents the interaction cost of the public

grid. The calculation of each cost is shown in (8) [21].

$$\begin{cases} C_f(t) = \sum_{i=1}^{N} C_{\text{fuel}} \times \frac{1}{\text{LHV}} \times \sum_{t=1}^{T} \frac{P_i(i)}{\eta_i(t)} \\ C_{i,\text{ma}}(t) = \sum_{i=1}^{N} MA_i(P_{i,t}) = \sum_{i=1}^{N} K_{MA_i,t} \times P_{i,t} \\ C_{i,\text{dep}}(t) = \sum_{i=1}^{N} DEP_i(P_{i,t}) = \sum_{i=1}^{N} \frac{\text{ADC}_i}{P_{N,i} \times 8760 \times cf_i} \times P_{i,t} \end{cases} \tag{8}$$

In (8), $C_f(t)$ is mainly the consumption cost of natural gas, C_{fuel} represents the price, which is 3.75 yuan/m^3. i counts micro power sources and LHV is the low calorific value at 9.7 kWh/m^3. $P_i(i)$ represents the output power of the i-th generation unit at time t, and $\eta_i(t)$ represents generation unit working efficiency. $C_{i,\text{ma}}(t)$ represents i-th unit maintenance management cost, $P_{i,t}$ represents i-th unit output power, and $K_{MA_i,t}$ represents the maintenance cost coefficient. $C_{i,\text{dep}}(t)$ represents i-th unit depreciation loss, ADC_i represents unit annual average depreciation cos, $P_{N,i}$ represents the maximum output power, and cf_i represents unit capacity factor. The objective function of operating cost when only environmental protection is considered is established based on the treatment cost of discharged pollutant gas, as shown in (9) [22].

$$\min C_2 = \sum_{t=1}^{T} \sum_{j=1}^{J} \alpha_j (\sum_{i=1}^{N} \beta_{\text{ij}} P_{\text{it}} + \beta_{\text{mj}} P_{\text{mt}}) \tag{9}$$

In (9), C_2 refers to the operation cost when only environmental protection is considered, that is, the treatment cost of harmful gases, such as CO, CO_2, SO_2, and NO_x, and α_j refers to the treatment cost of class J polluting β_{ij} and β_{mj}, respectively, represent the emission coefficient of class J pollution gas in Mg and large grid, and P_{it} and P_{mt} represent the actual working power of Mg and large grid. The objective function considering the economy and environmental protection is shown in (10) [23].

$$\begin{cases} \min C_3 = [C_1, C_2] \\ C_3 = \lambda_1 C_1 + \lambda_2 C_2 \\ \lambda_1 + \lambda_2 = 1 \end{cases} \tag{10}$$

In (10), $\min C_3$ represents the minimum operation cost considering the economy and environmental protection, and λ represents the weight coefficient. Since the electric energy generated by PV and WT is converted from renewable new energy, considering that the natural gas in MT is not renewable energy, the objective function for determining the energy consumption of MT is shown in (11) [24].

$$F(u_{i,t}, P_{i,t}) = \sum_{t=1}^{T} \sum_{i=1}^{N} (u_{i,t} F_i(P_{i,t}) \Delta t + u_{i,t}(1 - u_{i,t-1}) S_i) \tag{11}$$

In (11), $F(u_{i,t}, P_{i,t})$ represents the total natural gas consumption of all MT, $u_{i,t}$ indicates the working state of the i-th MT, with a value of 0 or 1, respectively, indicating off and on. S_i indicates the start and stop consumption of the i-th MT and $P_{i,t}$ is the i-th MT active power. Since

the Mg operation is not unconstrained, certain constraints can ensure the power balance and rationality of Mg, and the power balance constraints of the power grid are shown in (12) [25].

$$\begin{cases} \sum_{i=1}^{N} P_i(t) + P_{\text{bat}}(t) + P_{\text{grid}}(t) = P_l(t) \\ P_{\text{imin}}(t) \leq P_i(t) \leq P_{\text{imax}}(t) \end{cases} \quad (12)$$

In (12), $P_{\text{bat}}(t)$ refers to energy storage device power, $P_{\text{grid}}(t)$ is the power purchased from the public grid, and $P_l(t)$ is user load power. This indicates that $P_i(t)$ needs to be within a certain upper and lower limit to ensure that the power generation system is feasible. The ramp rate can represent the performance of the power generation unit. The ramp rate constraint of each unit in Mg is shown in (13) [26].

$$\begin{cases} |P_{i,\text{up}}(t) - P_{i,\text{up}}(t-1)| \leq R_{i,\text{up}} \cdot \Delta t \\ |P_{i,\text{down}}(t) - P_{i,\text{down}}(t-1)| \leq R_{i,\text{down}} \cdot \Delta t \end{cases} \quad (13)$$

In (13), $P_{i,\text{up}}(t)$ and $P_{i,\text{down}}(t)$ represent $P_i(t)$increased and decreased active power. $R_{i,\text{up}}$ and $R_{i,\text{down}}$ indicate the increase and decrease of the active power limit of $P_i(t)$, respectively. The line transmission power constraint between the Mg and distribution network is shown in (14) [27].

$$P_{\text{line,min}}(t) \leq P_{\text{line}}(t) \leq P_{\text{line,max}}(t) \quad (14)$$

In (14), $P_{\text{line,max}}(t)$ and $P_{\text{line,min}}(t)$ represent the maximum and minimum line transmission power, respectively. Excessive charging and discharging will reduce the service life of BAT, so the charging and discharging power are restricted, as shown in (15) [28].

$$\begin{cases} S_{\text{SOCmin}} \leq S_{\text{SOC}}(t) \leq S_{\text{SOCmax}} \\ P_{\text{BESSin}}(t) \leq P_{\text{BESSin,max}} \\ P_{\text{BESSout}}(t) \leq P_{\text{BESSout,max}} \end{cases} \quad (15)$$

In (15), $S_{\text{SOC}}(t)$ represents the state of BAT charge, and $P_{\text{BESSin}}(t)$ and $P_{\text{BESSout}}(t)$ represent charging and discharging power. The schematic diagram of the Mg combinatorial optimisation mathematical model is shown in Fig. 2.

3.3 Construction of Optimisation Problem Model Using Improved PSO

For objective function solutions, the optimisation algorithm is usually for calculation. Common optimisation algorithms include the ant colony algorithm, firefly algorithm, whale algorithm, PSO, *etc.* The core idea is to simulate the animal's behaviour for optimal solution. PSO simulates birds' foraging behaviour and realises the optimal cooperation mode between birds and bird groups to find food. To improve solution accuracy, SA is used to improve the PSO. SA algorithm simulates the annealing process of solid fuel and compares the combinatorial optimisation problem with the annealing process of solid fuel. The
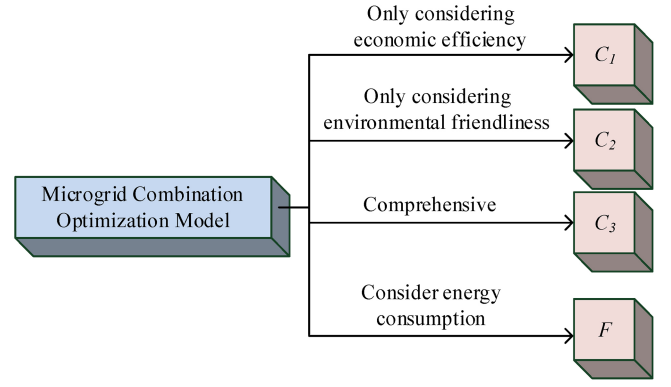
Figure 2. Schematic diagram of microgrid combination optimisation mathematical model.

iterative cycle process of the algorithm simulates the state that the internal energy of solid fuel reaches thermal equilibrium in the process of solid combustion and cooling. In the SA algorithm, with solid annealing, if the new solution offers greater value than the old solution, it will replace the old solution. However, if the new solution offers less value than the old solution, a suboptimal solution may be generated. The probability of outputting a poor solution is shown in (16) [29].

$$p = exp(-\frac{E(x_{\text{new}}) - E(x_{\text{old}})}{\text{kT}}) \quad (16)$$

In (16), k is the Boltzmann constant, T is the temperature, and $E(x_{\text{new}})$ and $E(x_{\text{old}})$ are the new solution and the old solution, respectively. From (16), the higher the temperature, the higher the probability of the algorithm selecting the worst solution. Therefore, the algorithm avoids falling into the local optimal solution. The flowchart of the SA algorithm is shown in Fig. 3.

To improve the PSO problem, the SA algorithm and PSO algorithm are combined to construct SAPSO. It uses the idea of probability jump in SA to realise the jump-out. In the SAPSO algorithm, the inertia weight parameter needs to be initialised first, and the calculation is shown in (17) [30].

$$\omega = \omega_{\text{max}} - (\omega_{\text{max}} - \omega_{\text{min}})(\frac{k}{k_{\text{max}}})^2 \quad (17)$$

In (17), ω represents the inertia weight, ω_{max} and ω_{min} represent the start value and end value of inertia weight, which can be set to 0.9 and 0.4 according to experience. k indicates the number of iterations and k_{max} is the max iteration [31], [32]. The fitness value of each particle is computed by evaluating its solution using a fitness function. This allows for the identification of both the optimal solution within each particle and the global optimal solution within the current population. SA initial temperature is obtained through the optimal fitness value. The initial temperature is shown in (18) [33].

$$T = -\frac{f(P_{\text{pd}})}{ln0.2} \quad (18)$$
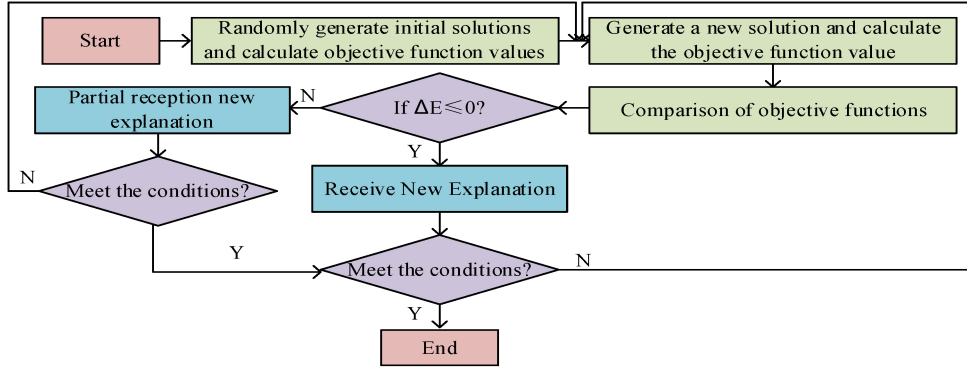
Figure 3. Flowchart of SA algorithm.
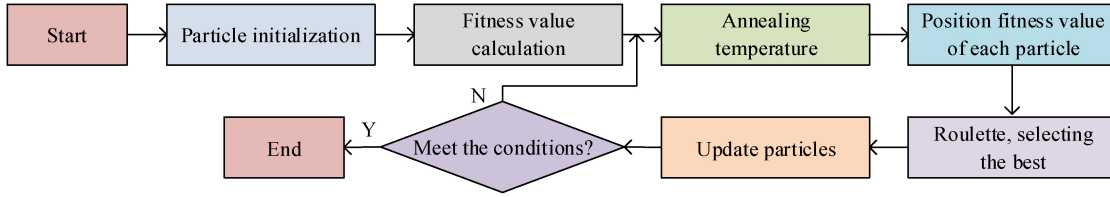
Figure 4. Flowchart of SAPSO algorithm.

(a)

(b)
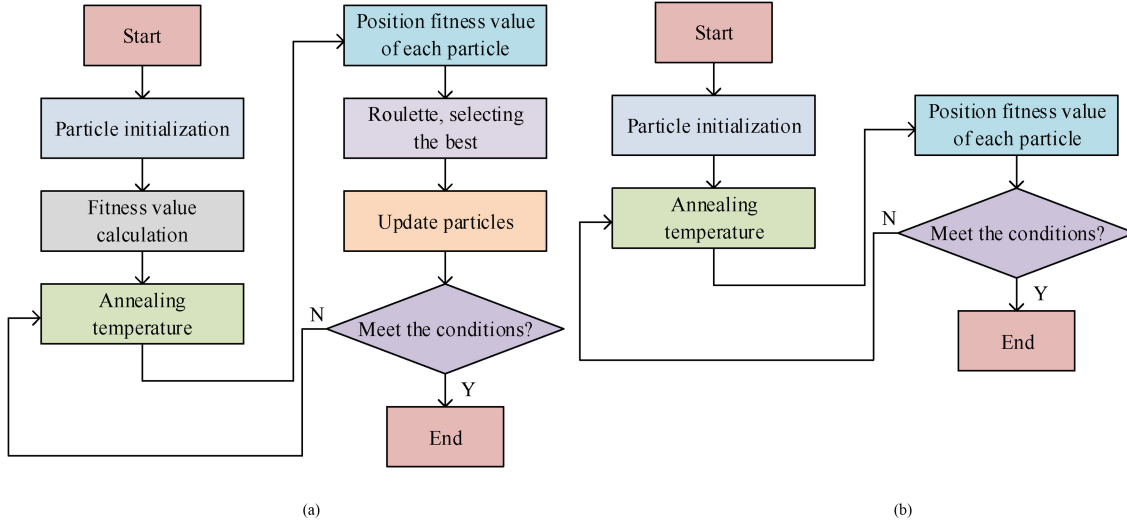
Figure 5. The difference between the improved SAPSO algorithm and the original one.

In (18), $f(P_{\mathrm{pd}})$ represents the fitness value of the optimal position. The roulette method can calculate the fitness value of each global optimal position under the current temperature. The fitness of the current solution is compared with the fitness of the global optimal solution. The global optimal solution is updated if the current solution achieves a higher fitness. The termination condition can be determined by either the number of iterations or the range of variation in solutions [34]. Once the termination condition is met, the global optimal solution is returned as the result. The flowchart of the SAPSO algorithm is shown in Fig. 4.

The difference between the improved SAPSO algorithm and the original one is shown in Fig. 5.

From Fig. 5, compared with PSO, SAPSO has added key links to dynamically adjust the performance of the current search stage or particles, which helps balance the ability of global search and local search. Meanwhile, SAPSO adopts an adaptive neighbourhood topology structure to improve information flow efficiency and promote knowledge sharing among different individuals within the group. SAPSO may allow particles to self-learn parameter values based on experience, without the need for algorithm designers to manually adjust them.

Table 1
Table of Treatment Costs for Relevant Parameters

Power supply type	Maximum power value	Minimum power value	Binding power	Fuel cost	Operating cost
PV	0	20	-	-	0.0096
Wt	0	80	-	-	0.0450
MT	0	50	80	0.358	0.0450
FC	0	60	60	0.199	0.0295
WIP	-30	30	-	0.147	0.0742
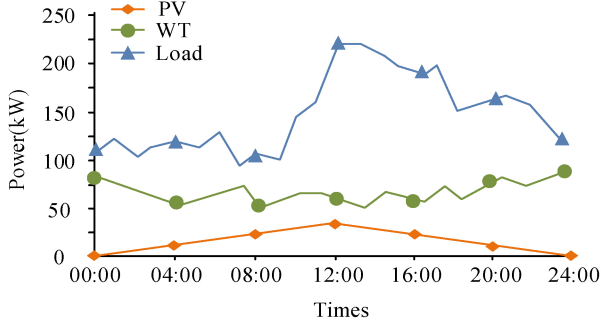
Figure 6. Prediction data of wind power, photovoltaic output, and user load.

Table 2
Table of Aggregates of Each Micro Power Supply

Types of pollutants	Emission factor	Process price		
	MT	FC	WIP	
CO_2	1.0782	1.5982	1.4350	26.4550
SO_2	0.0035	0.0080	0.4550	6.2350
NO_x	0.2000	0.0140	21.8000	0.0880

4. Experimental Analysis of Mg Combination Model

To study SAPSO performance in the Mg combinatorial optimisation model, this chapter is divided into two parts. The first part describes the background data and parameter settings of the selected Mg, and the second part tests and analyses the model.

4.1 Mg Data and Model Parameter Setting

To verify SAPSO algorithm effectiveness, this study used MATLAB system. The experiment took one day as a cycle, and PV and WT operated at maximum power. The energy storage device had a maximum charging and discharging power capacity of 10 kW. Furthermore, the power purchased from the public grid was limited to a maximum of 40% of the daily load. A city in China was selected as the experimental object. The electricity purchase price was 0.165 yuan/kwh and the electricity sale price was 0.130 yuan/kwh from 23:00 to 07:00. During the period from 06:00 to 12:00 and from 15:00 to 18:00, the power purchase price was 0.490 yuan/kwh and the power sale price was 0.380 yuan/kwh. The electricity purchase price was 0.830 yuan/kwh and the electricity sale price was 0.650 yuan/kWh at 12:00–15:00 and 18:00–23:00 in peak hours. By referring to the power consumption of the place, the predicted data are obtained as shown in Fig. 6.

In Fig. 6, the wind was small due to sufficient sunlight in the daytime. Therefore, the PV in this area reached

Figure 7. Iterative optimisation process of operating costs for four models.

the maximum power at 12:00 noon, and the power of WT at night was greater than that during the day. The relevant parameters of each micro power supply is shown in Table 1.

From Table 1, it can be seen that the maximum power values of PV, WT, MT, and FC are all 0, and the maximum power values of WIP are all -30. The minimum power values are 20, 801, 50, 60, and 30, respectively. The treatment cost of pollutants in the area is shown in Table 2.

From Table 2, the fuel cost and the operation cost for power supply were far less than the treatment cost of pollutants. Excessive use of fossil fuels reduced the cost but increase the pollutants, which cannot achieve the balance between economy and environmental protection. Therefore, intelligent optimisation algorithm can solve the objective problem in Mg.
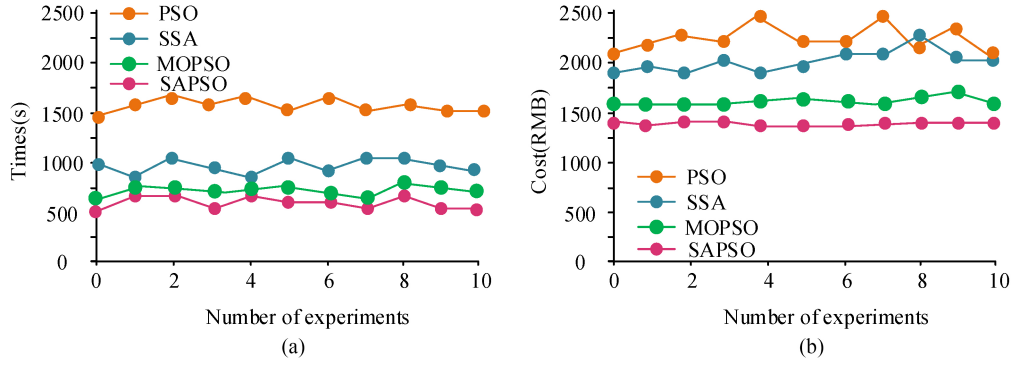
Figure 8. Average operation time of four models: (a) runtime and (b) cost comparison.

4.2 Model Case Analysis

The Mg system in a domestic city was selected as an example to analyse the Mg system in this region. The objective function was set as the Mg minimum operation cost considering the economy and environmental protection. Multi-objective particle swarm optimisation (MOPSO), SSA, PSO algorithm, and SAPSO algorithm were selected for comparison. MOPSO is specifically designed to solve multi-objective optimisation problems and can handle multiple objective functions simultaneously. The SSA algorithm is a heuristic optimisation algorithm inspired by the foraging behaviour of sparrows and designed to solve multi-objective optimisation problems, including the optimal scheduling problem of Mgs. Therefore, the SSA algorithm, as a typical heuristic optimisation algorithm, is particularly suitable for solving such complex problems. By comparing the performance of these algorithms, their application effectiveness, advantages, and disadvantages can be better evaluated in Mg system optimisation. The epoch of MOPSO, SSA, PSO, and SAPSO models was set to 300, and the initial particle number was set to 600. The start and end values of inertia weight were set to 0.9 and 0.4, and the learning factor to 1.0. The operation cost iterative optimisation process of the four models is shown in Fig. 7.

In Fig. 7, four models' operating costs decreased as iteration times increased. However, the PSO algorithm fell into the local optimal solution when the number of iterations was 80, 150, and 225. The SAPSO model tended to converge at 60 iterations, and the optimal operating cost was 1,500 RMB. The iteration curves of the SAPSO model and MOPSO model were very close, but SAPSO tended to stabilise 10 times earlier than MOPSO. The experiment was repeated 10 times and the average value of the 10 runs was calculated. The average operation time and cost of the four models were compared. At the same time, to compare the four algorithms' stability in solving the model, the total cost curve was drawn. The results are shown in Fig. 8.

Fig. 8(a) and 8(b) represents the time and cost of 10 runs, respectively. The horizontal axis represents the number of experiments, and the vertical axis represents time and cost. In Fig. 8, the PSO average operation time was 1,550 s, that of SSA was 980 s, the average running

time of MOPSO was 682 s, and that of SAPSO was 625 s. At the same time, the curve of the SAPSO algorithm to solve the cost fluctuated less and was relatively stable. SAPSO had faster running time and improved the speed of problem-solving. This meant that in practical applications, such as Mg optimisation scheduling, the SAPSO algorithm solved problems more efficiently, quickly obtained the optimal solution, and better ensured the stability of the solution. This provided more powerful optimisation tools for the actual operation and management of Mg systems. After 10 simulation experiments, the average cost, standard deviation, minimum value, and median value calculated by the four algorithms are shown in Table 3.

In Table 3, the average operating cost obtained by the SAPSO model was 1,458.52 RMB, the standard deviation was 75.49 RMB, the minimum cost was 1,355.06 RMB, and the median was 1,483.27 RMB. Because PSO was easy to fall into the local optimal solution, the calculated result was the most unsatisfactory. Compared with the PSO algorithm, the SSA algorithm was improved, but compared with the SAPSO algorithm, the SSA algorithm still had shortcomings. Although MOPSO performed better than SSA and PSO, its cost was still higher than SAPSO, indicating that MOPSO was not as cost-effective as SAPSO. It showed that the SAPSO model was stable, and the cost solution was optimal. The energy consumption calculated by SSA, PSO, MOPSO, and SAPSO models was compared and analysed, as shown in Fig. 9.

The horizontal axis in Fig. 9 represents the number of iterations, and the vertical axis represents the energy consumption situation. In Fig. 9, the SAPSO algorithm tended to converge after 25 iterations. MOPSO tended to converge after 50 iterations. The SSA algorithm converged after 95 iterations. The PSO algorithm converged after 148 iterations. Their minimum energy consumption values were 2.575×10^5 J, 2.605×10^5 J, 2.655×10^5 J, and 2.675×10^5 J. Therefore, the SAPSO algorithm can solve the minimum energy consumption value, and can effectively reduce the emission of pollutants in the Mg operation. The SAPSO algorithm shows high efficiency and accuracy in finding the minimum energy consumption value of Mgs. Compared to the SSA algorithm and PSO algorithm, it requires fewer iterations for convergence and obtains a lower minimum energy consumption value. This means that in actual

Table 3
Cost Results Calculated by Four Algorithms (Unit: RMB)

Algorithm name	SSA	PSO	MOPSO	SAPSO
Average value	2,045.55	2,320.15	1,862.31	1,458.52
Standard deviation	255.42	350.28	172.04	75.49
Minimum value	1,843.26	2,050.19	1,620.68	1,355.06
Median	2,050.92	2,370.55	1,742.31	1,483.27
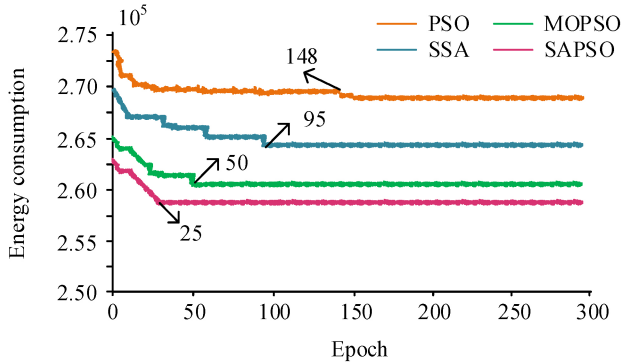
Figure 9. Energy consumption iterative optimisation process of three models.
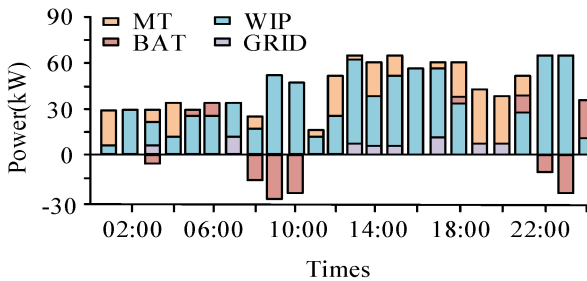
Figure 10. Distributed power sources output.

Mg operation, using the SAPSO algorithm for energy management and optimisation can more effectively reduce energy consumption, reduce environmental pollution, and improve the sustainable development ability of Mgs. Each distributed generation output optimised by the SAPSO model is shown in Fig. 10.

The horizontal axis in Fig. 10 represents time, and the vertical axis represents the output of distributed power sources. In the optimal dispatch of Mg, PV, and WT systems operated at maximum output. As can be seen from Fig. 9, BAT was in the discharge phase during the period of 00:00–06:00. At this stage, BAT, WIP, and MT cooperated to ensure the load demand. During the period of 08:00–12:00, renewable energy generation was mainly used to satisfy load, and BAT was in a state of charge. During the period from 13:00 to 20:00, the power demand
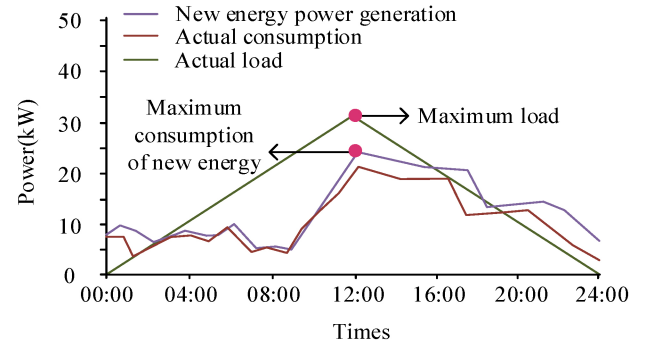
Figure 11. Consumption of new energy.

increased, and BAT discharge increased to meet the needs of users. During the 20:00–00:00, MT and WIP output increased, and BAT was in charge state. At low load demand, renewable energy sources, such as PV and wind power were mainly relied upon to meet the demand, while batteries were also used for energy storage. However, during peak electricity usage, the battery began to discharge to meet additional demand. This dynamic scheduling strategy helped balance and maximise the utilisation of various energy resources in Mg systems, ensuring that user needs were met at different periods, reducing reliance on traditional energy, and improving the reliability and economy of Mgs. The consumption of new energy is shown in Fig. 11.

In Fig. 11, during the power consumption peak period, the load was much larger than the power of new energy. At 12:00, the maximum load occurred, and the new energy consumption and actual value were 22.4 kW and 20.5 kW, respectively, indicating a good new energy consumption effect. The SAPSO algorithm can ensure that the new energy consumption rate of the Mg system can reach 100%, to achieve the effect of environmental protection and energy conservation.

5. Conclusion

To achieve the output balance of the Mg system and meet the comprehensive benefit demand of the Mg system dispatching under the new energy consumption. This research uses PSO and introduces SA and proposes an improved PSO for new energy consumption. The experimental results showed that PSO fell into the local optimal solution briefly when iterations were 80, 150, and 225. The SAPSO model tended to converge at 60 iterations, and the optimal operating cost was 1,500 yuan. The average operating cost of the SAPSO model was 1,458.52 RMB, the standard deviation was 75.49 RMB, the minimum cost was 1,355.06 RMB, and the median was 1,483.27 RMB. The average running time of PSO was 1,550 s, the average running time of SSA was 980 s, the average running time of MOPSO was 682 s, and the average running time of SAPSO was 625 s. PSO, SSA, MOPSO, and SAPSO tended to converge after 148, 95, 50, and 25 iterations, and the minimum energy consumption values obtained were 2.675×10^5 J, 2.655×10^5 J, 2.608×10^5 J, 2.575×10^5 J, respectively. The average operation time

of PSO was 1,550 s, that of SSA was 980 s, that of MOPSO was 682 s, and that of SAPSO was 625 s. Results showed good stability of SAPSO, and the cost solution was the best, which proved that the SAPSO model was superior to the PSO model in optimisation ability. At the same time, the SAPSO algorithm can ensure that the new energy consumption rate of the Mg system can reach 100% to achieve the effect of environmental protection and energy saving. This study has shortcomings, lack of optimisation for the model-solving speed, in the next study, more optimisation algorithms should be used to shorten the time. Efforts are being made to further optimise Mg management and new energy consumption. This includes the development and improvement of PSO algorithms that can adapt to different Mg scenarios. Research is also being conducted on the application of energy storage systems, along with the development of energy trading mechanisms across Mgs.

Fundings

References

[1] B. Zhou, J. Zou, and C.Y. Chung, Multi-microgrid energy management systems: architecture, communication, and scheduling strategies, *Journal of Modern Power Systems and Clean Energy, 9*(3), 2021, 463–476.

[2] K. Rajesh and R. Jenitha, Radial basis function neural network MPPT controller-based microgrid for hybrid stand-alone energy system used for irrigation, *Circuit World, 49*(2), 2023, 251–266.

[3] T. Le and B.L.N. Phung, Load shedding in microgrids with consideration of voltage quality improvement, *Engineering, Technology and Applied Science Research, 11*(1), 2021, 6680–6686.

[4] C. Ndukwe, M.T. Iqbal, and X. Liang, LoRa-based communication system for data transfer in microgrids, *AIMS Electronics and Electrical Engineering, 4*(3), 2020, 303–325.

[5] C. Cepeda, C. Orozco, and W. Percybrooks, Intelligent fault detection system for microgrids, *Energies, 13*(5), 2020, 1223.

[6] D. An, Q. Yang, and W. Yu, LoPrO: Location privacy-preserving Online auction scheme for electric vehicles joint bidding and charging, *Future Generation Computer Systems, 107*(6), 2020, 394–407.

[7] E. Masuda, Y. Matsuda, and Y. Wakasa, Solution to DC optimal power flow problems with demand response via distributed asynchronous primal-dual algorithms, *SICE Journal of Control Measurement and System Integration, 13*(3), 2020, 66–72.

[8] S. Ghaemi and J. Salehi, Assessment of flexibility index integration into the expansion planning of clean power resources and energy storage systems in modern distribution network using benders decomposition, *IET Renewable Power Generation, 14*(2), 2020, 231–242.

[9] R. Krishna, H. Sathish, and N. Zhou, Forecasting uncertainty parameters of virtual power plants using decision tree algorithm, *Electric Power Components and Systems, 51*(16), 2023, 1756–1769.

[10] S. Zeinal-Kheiri, S. Ghassem-Zadeh, and A.M. Shotorbani, Real-time energy management in a microgrid with renewable generation, energy storages, flexible loads and combined heat and power units using Lyapunov optimisation, *IET Renewable Power Generation, 14*(4), 2020, 526–538.

[11] X. Wu, Y. Yang, S. Han, Z. Zhao, P. Fang, and Q. Gao, Multi-objective optimization method for nuclear reactor radiation shielding design based on PSO algorithm, *Annals of Nuclear Energy, 160*, 2021, 108404.1–108404.12.

[12] M. Abbaszadeh, S. Soltani-Mohammadi, and A.N. Ahmed. Optimization of support vector machine parameters in modeling of IJU deposit mineralization and alteration zones using particle swarm optimization algorithm and grid search method. *Computers & Geosciences, 165*, 2022, 105140.1–105140.13.

[13] Y. Chen, Z. Ding, M. Zhang, J. Zhou, M. Li, M. Zhao, and J. Wang, Metasurface parameter optimization of Fano resonance based on a BP-PSO algorithm, *Applied Optics, 60*(29), 2021, 9200–9204.

[14] S. Singh, P. Chauhan, and N.J. Singh, Capacity optimization of grid connected solar/fuel cell energy system using hybrid ABC-PSO algorithm, *International Journal of Hydrogen Energy, 45*(16), 2020, 10070–10088.

[15] A.M. Shaaban, C. Anitescu, E. Atroshchenko, and T. Rabczuk, Shape optimization by conventional and extended isogeometric boundary element method with PSO for two-dimensional Helmholtz acoustic problems, *Engineering Analysis with Boundary Elements, 113*, 2020, 156–169.

[16] M. Ren, X. Huang, X. Zhu, and L. Shao, Optimized PSO algorithm based on the simplicial algorithm of fixed point theory, *Applied Intelligence, 50*(7), 2020, 2009–2024.

[17] M.A. Memon, M. Daula, S. Mekhilef, and M. Mubin, Asynchronous particle swarm optimization-genetic algorithm (APSO-GA) based selective harmonic elimination in a cascaded H-bridge multilevel inverter, *IEEE Transactions on Industrial Electronics, 69*(2), 2022, 1477–1487.

[18] X. Ji, B. Yang, and Q. Tang, Acoustic seabed classification based on multibeam echosounder backscatter data using the PSO-BP- adaboost algorithm: A case study from Jiaozhou Bay, China, *IEEE Journal of Oceanic Engineering, 46*(2), 2020, 509–519.

[19] Y. Yan, Z. Fan, G. Sun, and K. Tian, Diffractive optical element design based on vector diffraction theory and improved PSO-SA algorithm, *Optical Engineering, 62*(2), 2023, 025103.1–025103.12.

[20] V.B. Mazza, R. Bustamante, A.R.F.D.A. Martins, L.A.C. Teixeira, and B.F.D. Santos, Modelling and optimization of the ferrous to ferric sulphate conversion with hydrogen peroxide using polynomial-PSO and PSO-ANNs models, *The Canadian Journal of Chemical Engineering, 100*(12), 2022, 3653–3668.

[21] M. Raeispour, H. Atrianfar, and H.R. Baghaee, Resilient distributed control of BESSs and VSC-based microgrids considering switching topologies and nonuniform time-varying delays, *IET Generation Transmission & Distribution, 14*(22), 2020, 5060–5071.

[22] S.S. Bohra, Anvari-A. Moghaddam, and F. Blaabjerg, Multi-criteria planning of microgrids for rural electrification, *Journal of Smart Environments and Green Computing, 1*(2), 2021, 120–134.

[23] X. Ma, X. Zhang, and X. Zhao, Service coverage optimization for facility location: considering line-of-sight coverage in continuous demand space, *International Journal of Geographical Information Science, 37*(7), 2023, 1496–1519.

[24] N.H. Son, Solution stability to parametric distributed optimal control problems with finite unilateral constraints, *Evolution Equations and Control Theory, 11*(4), 2022, 1357–1372.

[25] J. Zhai, M. Zhou, and J. Li, Decentralised and distributed day-ahead robust scheduling frameworks for bulk AC/DC hybrid interconnected systems with a high share of wind power, *Electric Power Systems Research, 201*(6), 2021, 107492–107492.

[26] L. Guo and N.M.M. Abdul, K. Wang, Design and implementation of virtual laboratory for a microgrid with renewable energy sources, *Computer Applications in Engineering Education, 30*(2), 2022, 349–361.

[27] Q. Hassan, M. Jaszczur, and S.A. Hafedh, Optimizing a microgrid photovoltaic-fuel cell energy system at the highest renewable fraction, *International Journal of Hydrogen Energy, 47*(28), 2022, 13710–13731.

[28] A. Tabak, Fractional order frequency proportional-integral-derivative control of microgrid consisting of renewable energy sources based on multi-objective grasshopper optimization algorithm, *Transactions of the Institute of Measurement and Control, 44*(2), 2022, 378–392.

[29] H. Chen, W. Wang, X. Chen, and L. Qiu, Multi-objective reservoir operation using particle swarm optimization with adaptive random inertia weights, *Water Science and Engineering, 13*(02), 2020, 58–66.

[30] X. Sun, W. Hu, and X. Xue, Multi-objective optimization model for planning metro-based underground logistics system network: Nanjing case study, *Journal of Industrial and Management Optimization, 19*(1), 2023, 170–196.

[31] D. Gong and G. Li, Research on multi-objective optimized target speed curve of subway operation based on ATO system, *International Core Journal of Engineering, 6*(2), 2020, 133–137.

[32] Q. Huo and J. Guo, Multi-objective closed-loop logistics network model of fresh foods based on improved genetic algorithm*, Journal of Computer Applications, 40*(5), 2020, 1494–1500.

[33] J. Zan, Research on robot path perception and optimization technology based on whale optimization algorithm, *Journal of Computational and Cognitive Engineering, 1*(4), 2022, 201–208.

[34] M. Barma and U.M. Modibbo, Multiobjective mathematical optimization model for municipal solid waste management with economic analysis of reuse/recycling recovered waste materials*, Journal of Computational and Cognitive Engineering, 1*(3), 2022, 122–137.

Diangang Hu received the master's degree from North China Electric Power University. He also obtained Senior Engineer with the rank of a Professor, served with State Grid Gansu Electric Power Company. His main research direction is power system automation.

Lijuan Liu received the master's degree. Presently, she is working with State Grid Gansu Electric Power Research Institute. She mainly engaged in the analysis and calculation of new energy consumption.

Biographies

Guodong Wu received the master's degree in electrical engineering (2017) from the College of Electrical and Information Engineering, Lanzhou University of Technology. He also obtained National Certified Electrical Engineer, served with State Grid Gansu Electric Power Company. His research interests include renewable energy power generation and automation of electric power system.

Guangqing Bao received the M.S. degree in power electronics and power transmission from Gansu University of Technology, Lanzhou, China, in 2002, and the Ph.D. degree in power electronics and power transmission from Shanghai University, Shanghai, China, in 2006. He is currently working as a Professor with the School of Electrical and Electronic Engineering, Southwest Petroleum University. Her research interests include intelligent planning of power systems, risk assessment, and power communication systems.